1   # Investigation of ship cooling system operation for improving energy efficiency

2   **Gerasimos Theotokatos[1*], Konstantinos Sfakianakis[2] and Dracos Vassalos[1]**

3   1. Department of Naval Architecture, Ocean and Marine Engineering, University of Strathclyde, G4 0LZ, Glasgow, UK
4   2. Department of Electronic and Electrical Engineering, University of Strathclyde, G1 1XW, Glasgow, UK
5   * Corresponding author: Tel.: +44(0)1415483462   e-mail address: gerasimos.theotokatos@strath.ac.uk

6
7
8   **Abstract**
9
10 The application of recently introduced IMO regulations for reduction of CO_2 gaseous emissions as well as the initiatives

11 for greener shipping, rendered the efforts for improving on-board energy systems performance to be of high priority.

12 This study focuses on the investigation of the on-board operation of the combined sea/fresh water cooling system of a

13 merchant ship. The detailed model of a cooling system is presented based on energy and mass conservation laws. The

14 simulation input data includes the system geometry and arrangement, the operational characteristics of cooling pumps,

15 the control scenarios for the system valves as well as data for calculating the pipes friction and minor losses coefficients,

16 wherefrom the system performance parameters can be calculated. The cooling system energy consumption was

17 estimated considering a typical annual ship operational profile. Two cases were investigated; first, a conventional case

18 of controlling the sea water and fresh water temperatures by using three-way valves and, second, a more sophisticated

19 case of installing variable speed motors for driving the system pumps. The obtained results are compared in terms of

20 annual power consumption leading to conclusions about the system performance. The developed models can be used as

21 an assessment tool for improving shipboard power demand early in the design stage and, also, during operation.

22

25

1 Introduction

The last decade, ships energy efficiency and environmental performance have been of highest importance in shipping industry due to the fuel oil prices increase and the stringent emissions legislation concerning greenhouse gas emissions [1]. In this respect, the shipping industry has intensified its efforts for reducing ships energy consumption and gas emissions. Inevitably, the area of interest for many research groups and industry is focused on the performance improvement of the major on-board energy consumers, i.e. propulsion plants, hull/propeller etc. However, the ship auxiliary systems have not been attracted much attention, since their contribution to the total energy consumption is substantially lower than the respective one of the ship propulsion system.

The majority of the ship electrical energy utilisers include pumps, compressors and fans/blowers. Since the ship cooling systems usually comprise the largest ship pumps and operate for the majority of the ship lifetime, they are considered of vital importance in terms of improving the ship energy efficiency. Presently, the standard design methods for the cooling systems are based on considering the worst case scenarios e.g. tropical conditions and all the ship engines/machinery operating at their maximum load. As a consequence, the installed on-board systems are oversized and in turn, they demand a significantly greater amount of energy. Therefore, there is enough space for energy efficiency improvement at the design stage as well as during operation considering the introduction of new available technologies, such as variable frequency drives [2].

The typical pumps that are used by the shipping industry work at a constant speed under the rated (nominal) frequency (usually 60 Hz) without taking into consideration the real system thermal power needs. In addition, the on-board system fluid flow control is performed with the use of bypass branches and/or throttling valves [2]. It is inevitable that the commonly used techniques end up to the system inefficient operation and therefore, energy saving technologies can be utilized as potential solutions [2-3]. In this respect, the pump motor speed control using Variable Frequency Drives (VFD) might be an effective solution that has not been adapted yet to a great extent in the shipping industry [4]. The energy saving is based on the concept of reducing the system operating pumps speed, and therefore, lowering the required power demand for the cases where the system operates in lower heat capacity conditions , which can be accommodated by reducing the cooling water flow rate.

Despite the importance of the applying energy saving technologies in ship systems, only limited published works have been found dealing with modelling, control and energy savings for the ship cooling system. In [5], a model capable of predicting the transient response of a merchant ship cooling system was developed and verified against measured data. Subsequently, it was used for investigating the influence of the controller parameters on the system behaviour. In [6], a similar methodology was followed to develop an appropriate linearised model capable of predicting the transient

response of a containership cooling system. Based on this, two different control designs were investigated under various

operating conditions for controlling the sea water and fresh water temperature. In [3], the energy savings that can be

achieved by using a VFD on the cooling system pumps of two different ships were investigated considering fixed

thermal energy demand and varying sea water temperature for the ship voyages throughout the period of one year. In

this respect, further studies on the integrated sea water-fresh water cooling system investigation that consider the

varying operating conditions and actual ship engines operating profiles are quite useful for providing insight to the

overall system operation and the expected benefits for applying energy saving techniques.

The aim of this study is to realistically estimate the annual energy consumption of the integrated sea water/fresh water

cooling system of a typical handymax bulk carrier for two different operation methods, namely constant speed and

variable speed pump operation. The system was modelled by applying the energy and mass conservation equations in its

components, whereas a typical annual operating profile was considered for the ship main and auxiliary engines. The

model results, which include the head, volumetric flow rate and temperature of all system braches, as well as the pumps

required power, were analysed and the ship annual energy saving potential was discussed.

2 System Description

Typical ship cooling water systems consist of three parts: the sea water (SW) cooling system, the low temperature (LT)

fresh water cooling system and the high temperature (HT) fresh water cooling system, as shown in Figure 1. Since the

seawater causes corrosion issues, fresh water is used for cooling the ship main and auxiliary machinery. Thus, one or

more central coolers are installed on-board for cooling the hot fresh water exiting the ship machinery and heat

exchangers by using sea water.

The seawater system comprises a number of water pumps connected in parallel. Usually two main pumps (one

operating and one standby) and one smaller pump for operation at harbour are required; however three same main

pumps could also be used provided that the two pumps have to supply the cooling water flow rate required to cover the

design point operation (maximum flow rate scenario) [7]. The pumps function is to provide sea water to the central

cooler(s) in order to remove the required heat from the fresh water. The sea water system pumps have to maintain the

required flow rate and to provide the pressure increase required for covering the system pressure losses (induced to the

system pipe lines, fittings and components) and the elevation of sea water. For the case where the pump operates at

constant speed, the sea water flow rate is almost constant (although it depends on the system valves settings and the

components fouling/corrosion condition), and therefore the temperature of the sea water exiting the central cooler varies

with the cooler heat capacity, which depends on the serviced systems operating conditions. For the case where variable

86 pump speed is used, the pump speed can be adjusted, so that the sea water flow matches the actual central cooler heat

87 capacity and thus, the temperature of the sea water exiting the central cooler can be kept constant.
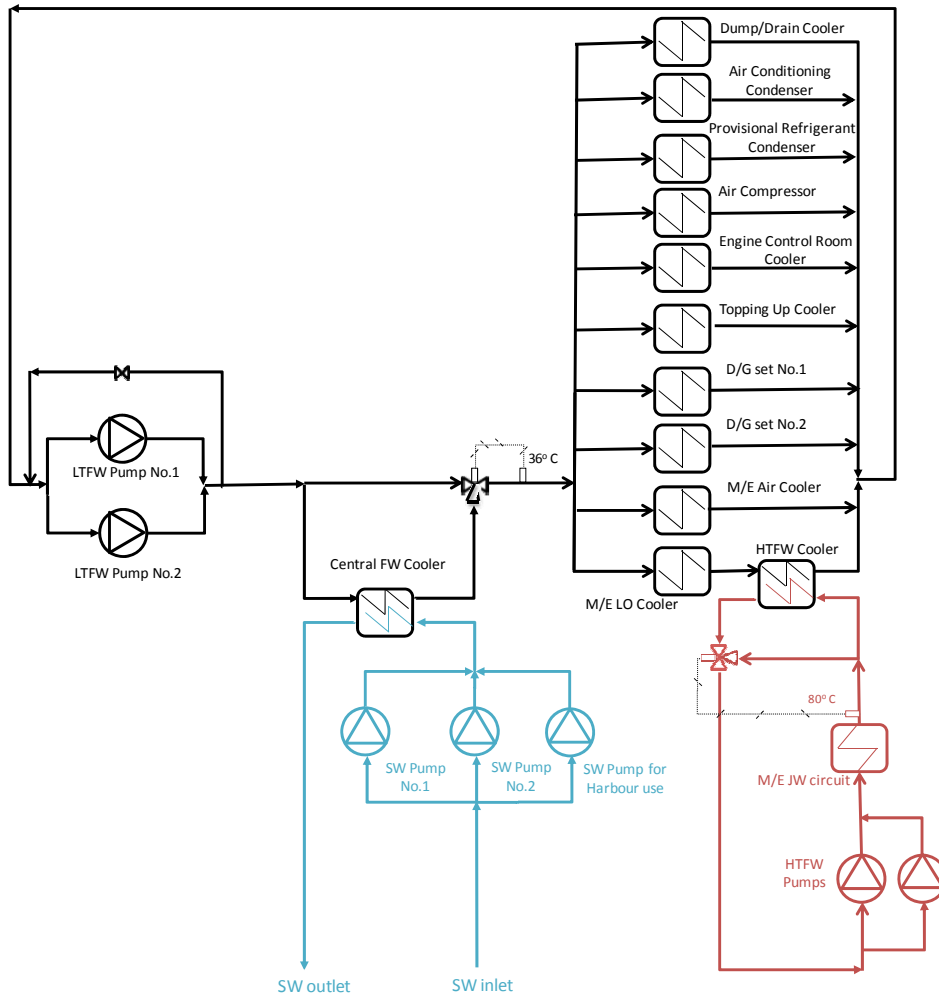
88

89   Figure 1: Bulk carrier integrated sea water/fresh water cooling water system diagram

90 The LT fresh water cooling system employs two (three in some cases) pumps [7] to service the main engine (M/E)

91 (scavenging air cooler, lubricating oil cooler and HT fresh water cooler) and the auxiliary machinery components

92 (Diesel-Electric generator (D/G) sets, air compressor, topping up cooler, dump drain cooler etc.). The temperature of the

93 fresh water entering the system coolers is controlled by a three-way valve, which is continuously adjusted to maintain

94 the temperature level at $36^{\circ}C$. When the system operating conditions differ from the system design point (less heat has

95 to be removed), the three-way valve mixes a flow at a lower temperature exiting from central cooler and a hotter

96 by-pass flow (returning from system coolers and components). That is required since the low temperature fresh water

97 pumps operate in constant speed and therefore, their flow rate does not depend on the serviced machinery instantaneous

98 heat capacity. On the other hand, in the case of the variable pump speed, the flow rate can match the actual needs of the

99 system and therefore, the three-way valve can remain in a position where the by-pass flow is zero.

100 The HT fresh water cooling system uses two pumps connected in parallel (one operates whilst the other remains standby)

4

101   to provide water for cooling the engine metallic parts (jacket cooling water circuit). For the pump constant speed

102   operation, the temperature of the water exiting the engine is indirectly adjusted to around 80°C (as proposed by the

103   engine manufacturer, although this depends on the engine settings) by using a three-way valve that mixes a water flow

104   at lower temperature exiting the HT fresh water cooler and the hot water flow exiting the engine. This is not required for

105   the case of variable speed pump, where the pump speed is adjusted, so that the water flow exiting the engine is kept at

106   the required temperature of 80°C.

107

108   3 System modelling

109   In this work, the steady state operation of the integrated system of sea water/fresh water cooling system that is shown in

110   Figure 2 was modelled. The governing equations were derived by applying the continuity equation in the system nodes,

111   the extended Bernoulli equation in the system branches and the energy conservation equation in the system heat

112   exchangers/coolers.
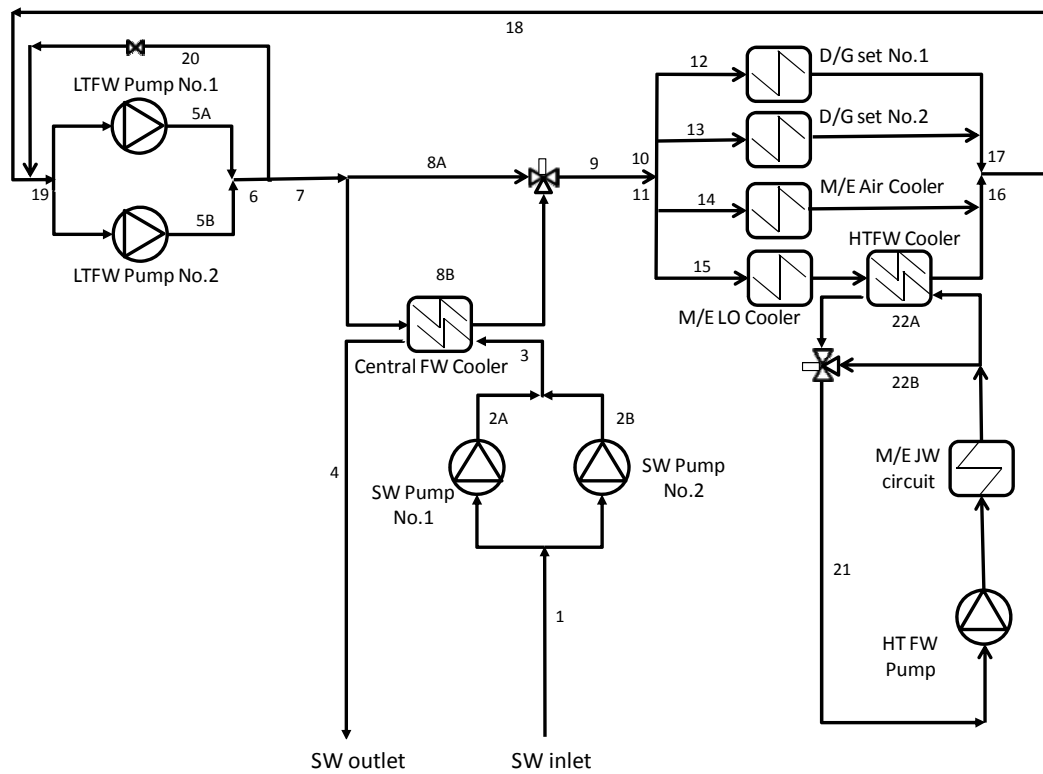
113

114   Figure 2: Modelled cooling water system layout

115   The head loss (in meters) of the system branches is calculated by taking into account the friction loss and the fittings

116   loss (valves, elbows, etc.) according to the following equation:

117        $$\Delta h_{loss,i} = \left(f_i \frac{L_i}{D_i} + \Sigma K_i \right) \frac{\dot{V}_i^{\,2}}{2gA_i^{\,2}} \qquad\qquad (1)$$

118 where i denotes the ith branch, f is the friction factor, L is the pipe length, D is the pipe hydraulic diameter, ΣK is the sum

119 of loss coefficients of the fittings along the considered branch, g is the gravitational acceleration, $\dot{V}$ is the volumetric

120 flow rate and A is the pipe internal cross-section area.

121 The friction factor is a function of Reynolds number for the laminar flow mode, whilst it can be calculated as a function of

122 Reynolds number and the relative roughness for the turbulent flow mode by using various equations of implicit or explicit

123 form. In this work, the Haaland equation [8] was used for calculating the friction factor as it has low computational cost

124 and adequate accuracy exhibiting a maximum error of 1.4% according to [9]:

125
$$f^{-0.5} = -1.8 \, log_{10} \left[\left(\frac{e/D}{3.7} \right)^{1.11} + \frac{6.9}{Re} \right] \qquad (2)$$

126 where e/D denotes the relative roughness and Re is Reynolds number.

127 The head loss of each cooler is calculated by using the following equation:

128
$$\Delta h_{HE,j} = K_{HE,j} \dot{V}_j^2 \qquad (3)$$

129 where j denotes the jth heat exchanger, K_{HE} is the heat exchanger loss coefficient and $\dot{V}$ is the volumetric flow rate.

130 The heat exchanger loss coefficient can be calculated based on the heat exchangers manufacturers' data or the methods

131 reported in [10]. Typical values for the maximum (permitted) pressure drop lay in the range from 0.7 to 1 bar at the

132 nominal flow point [10-11].

133 The head increase of each pump (in meters) is usually expressed in the form of the pump characteristic curves, in which

134 the pump head is plotted against the volumetric flow rate. For the case of centrifugal pumps, a second order polynomial

135 equation can represent the pump characteristic curve. Thus, the pump head is calculated according to the following

136 equation:

137
$$\Delta h_{p,i} = a\dot{V}_i^2 + b\dot{V}_i + c \qquad (4)$$

138 where i denotes the ith pump, $\dot{V}$ is the pump volumetric flow rate and a, b, c are constants.

139 For each heat exchanger, the energy conservation provides the following equation:

140
$$\dot{Q}_{HE} = \dot{V} \rho c_p \left(T_o - T_{in} \right)\Big|_{cold} = \dot{V} \rho c_p \left(T_{in} - T_o \right)\Big|_{hot} \qquad (5)$$

141 where $\dot{Q}_{HE}$ is the heat transferred from the hot fluid to the cold fluid, ρ is the fluid density, c_p is the fluid specific heat at

142 constant pressure, T_{in} is the fluid inlet temperature and T_{out} is the fluid outlet temperature.

143 Considering that there is no heat losses on the system heat exchangers, the energy balance results in the following

144 equations:

145
$$\dot{Q}_{CC} = \sum \dot{Q}_{LT,i}, \quad \dot{Q}_{HTFW} = \dot{Q}_{ME,JW} \qquad (6)$$

146   where i denotes the ith heat exchanger of the LT cooling system, $\dot{Q}_{CC}$ is the central cooler heat capacity, $\dot{Q}_{LT,i}$ is the heat

147   capacity of ith heat exchanger of LT cooling system, $\dot{Q}_{HTFW}$ is the HTFW cooler heat capacity and $\dot{Q}_{ME,JW}$ is the M/E

148   jacket water circuit heat capacity.

149   The extended Bernoulli equation applied to the system branches provides the formulas given below.

150   *Sea Water cooling system*

151

$$\Delta h_{p,2A} - \Delta z - \sum_{i=1\div4} \Delta h_{\text{loss},i} - K_{CC}\dot{V}_3^2 = 0 \qquad (7)$$

152   When the LT fresh water pumps operate simultaneously the following equation has to be additionally taken into account:

153

$$\Delta h_{p,2A} - \Delta h_{\text{loss},2A} - \Delta h_{p,2B} + \Delta h_{\text{loss},2B} = 0 \qquad (8)$$

154   *Low Temperature fresh water cooling system*

155

$$\Delta h_{p,5A} - \sum_{\substack{i=5A,6-7,8A,9-10,\\12,17-19}} \Delta h_{\text{loss},i} - K_{HE,12}\dot{V}_{12}^2 = 0 \qquad (9)$$

156

$$\Delta h_{\text{loss},12} + K_{HE,12}\dot{V}_{12}^2 - \Delta h_{\text{loss},13} - K_{HE,13}\dot{V}_{13}^2 = 0 \qquad (10)$$

157

$$\Delta h_{\text{loss},10} + \Delta h_{\text{loss},12} + K_{HE,12}\dot{V}_{12}^2 + \Delta h_{\text{loss},17}$$
$$- \Delta h_{\text{loss},11} - \Delta h_{\text{loss},14} - K_{HE,14}\dot{V}_{14}^2 - \Delta h_{\text{loss},16} = 0 \qquad (11)$$

158

$$\Delta h_{\text{loss},14} + K_{HE,14}\dot{V}_{14}^2 - \Delta h_{\text{loss},15}$$
$$- (K_{HE,15} + K_{HTFW})\dot{V}_{15}^2 = 0 \qquad (12)$$

159

$$\Delta h_{\text{loss},8A} - \Delta h_{\text{loss},8B} = 0 \qquad (13)$$

160

$$\Delta h_{\text{loss},19} + \Delta h_{\text{loss},5A} + \Delta h_{\text{loss},i6} - \Delta h_{\text{loss},20} = 0 \qquad (14)$$

161

$$\Delta h_{p,5A} - \Delta h_{\text{loss},5A} - \Delta h_{p,5B} + \Delta h_{\text{loss},5B} = 0 \qquad (15)$$

162   *High Temperature fresh water cooling system*

163

$$\Delta h_{p,21} - \sum_{i=21,22A} \Delta h_{\text{loss},i} - K_{HTFW}\dot{V}_{22A}^2 - K_{ME,JW}\dot{V}_{21}^2 = 0 \qquad (16)$$

164

$$\Delta h_{\text{loss},22A} - \Delta h_{\text{loss},22B} = 0 \qquad (17)$$

165   The continuity equation applied in each system node and considering incompressible flow gives the following equations:

166

$$\sum \dot{V}_i = 0 \qquad (18)$$

167   In the nodes where mixing of two flows occurs, the energy conservation provides the following equation:

168

$$\dot{V}_{in,1}\rho_{in,1}c_{p,in,1}T_{in,1} + \dot{V}_{in,2}\rho_{in,2}c_{p,in,2}T_{in,2} = \dot{V}_o\rho_o c_{p,o}T_o \qquad (19)$$

169   *Pumps power calculation*

170 The electric power that is needed for the pumps operation is calculated according to the following equation [12]:

171 $$P_{el,i} = \rho g \, \dot{V}_{p,i} \, \Delta h_{p,i} / \eta_i \qquad (20)$$

172 where i denotes the ith pump, η is the pump assembly efficiency that includes the pump, the motor and the variable speed

173 drive efficiencies, i.e.:

174 $$\eta_i = \eta_{p,i} \, \eta_m \, \eta_d \qquad (21)$$

175 The motor and drive efficiencies can be estimated according to the data provided in [13]. The considered variable speed

176 drive efficiency as a function of its load percentage is shown in Figure 3. The maximum pump efficiency was estimated

177 based on the volumetric flow rate and specific speed [12]. Then, the pump efficiency as function of its volumetric flow

178 rate was estimated using the maximum pump efficiency, the specific speed and the normalised diagrams provided in [14].

179 In order to estimate the pump characteristic at a speed value different that the pump rated speed, the affinity laws were

180 used [15]. According to them, similar operating points will exhibit the same efficiency and the volumetric flow rate, head

181 and speed are related using the following equations:

182 $$\dot{V}_1 / \dot{V}_2 = N_1 / N_2, \quad h_1 / h_2 = \left(N_1 / N_2 \right)^2 \qquad (22)$$

183 where 1 and 2 denote two similar points at pump speed N_1 and N_2, respectively.

184 Since the maximum pump efficiency is reduced at speed values different from the rated speed, the correction factor shown

185 in Figure 4 was applied for calculating the maximum pump efficiency [14].

186
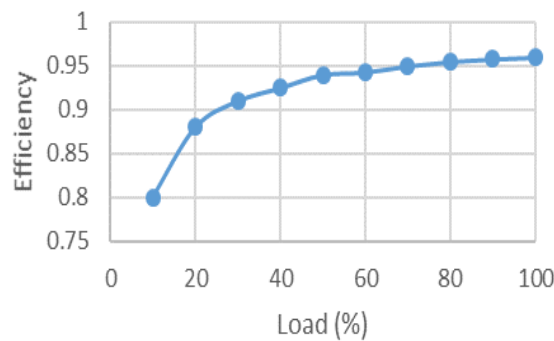
188 Figure 3: Variable speed drive efficiency as function of its load percentage
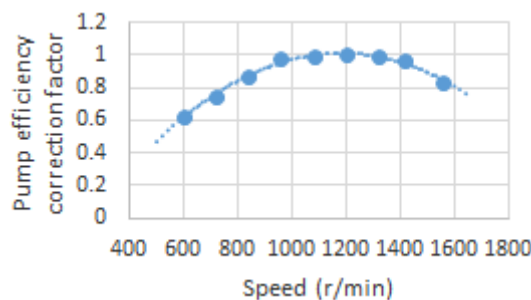
189
190 Figure 4: Pump efficiency correction factor

191

192   The equations (1)-(22) were simultaneously solved in MATLAB computational environment by using the "fsolve"

193   function. For all the system coolers, the constraint that the terminals temperature difference has to be kept greater that

194   5°C as proposed in [16] was taken into account.

195   The developed algorithm inputs include:

196   • Volumetric flow rate, head and speed at the pumps design operating points.

197   • Heat capacity of the system consumers (heat exchangers/main engine jacket cooling water circuit).

198   • Head loss coefficients for heat exchangers.

199   • Internal or hydraulic diameter of the pipes.

200   • Branches length.

201   • Number and type of fittings at each branch.

202   • Temperature set points for the system three way valves.

203   • Sea water temperature.

204   • Properties of the working fluid.

205   • Sea water elevation.

206   • Motors and variable speed drive efficiencies.

207   • Pumps operating speed.

208   The systems outputs include:

209   • The volumetric flow rate at each branch.

210   • The water temperature at each branch.

211   • The operating points (volumetric flow rate, head and efficiency) of each operating pump.

212   • The required electric power of each operating pump.

213

214   **4 Case studies**

215   The integrated sea water/fresh water cooling system of a typical handymax bulk carrier of 52,000 mt deadweight was

216   investigated by using the modelling approach described in the previous section. The ship uses a two-stroke marine

217   Diesel engine for propulsion that delivers 11,600 kW at its MCR point. In addition, two Diesel generator sets of 500 kW

218   each are used for supplying the required ship electric energy. The characteristics of the pumps servicing the sea water

219   and LT/HT fresh water cooling systems at their nominal operating points are presented in Table 1.

220   The integrated cooling system operation was simulated at various M/E operating conditions and considering that two

221   D/G sets operate at 55% load, which can provide the maximum ship electric power demand. It must be noted that the

222   majority of the ship operation, one D/G set can cover the ship electric power demand, however the assumption of two

223   operating D/G sets was considered in order to take into account a more demanding scenario for the operation of the ship

224   cooling system. Various scenarios were considered for the cooling system pumps including the pumps operation at fixed

225   speed, the pumps speed control and setting two different constraints for the temperature difference at the system heat

226   exchangers sides.

227   In addition, the annual required energy was estimated for each scenario based on the annual engine operating profile

228   according to the data presented in [17] for a similar size vessel and shown in Figure 5. The annual energy is calculated

229   by using the following equation:

230
$$E_a = H_a \sum_{j=1}^{n} \left(\frac{POT_j}{100} \sum_{i=1}^{k} P_{el,i} \right) \qquad (22)$$

231   where H_a denotes the annual operating hours, POT denotes the percentage of time the main engine operates at the

232   specific load, j denotes the different engine load points according to the considered profile, and i denotes the operating

233   pumps of the ship cooling system at each main engine load.
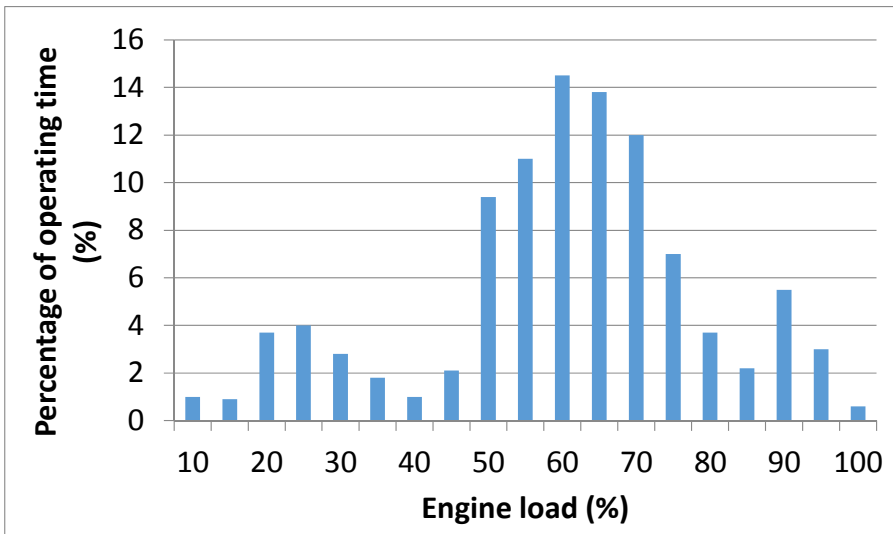
234

235   Figure 5: Ship main engine operating profile used for calculating the annual energy demand taken from [17]

236   The main engine and D/G sets heat capacities were obtained by the manufactures project guides [18, 19]. The cooling

237   systems characteristics were estimated based on the ship piping systems drawings and the list of machinery. An amount

238   of 4% losses for additional equipment losses (heat, cabling, etc.) was included in the calculations. In all the examined

239   cases herein, the temperature of sea water entering the central cooler was considered to be 25°C, whereas the set points

240   of the LT and HT three-way valves were taken as 36°C and 80°C, respectively. As the cooling system should be able to

241   cover the main engine and ship machinery requirements under varying conditions (from arctic to tropic; from low loads

242   to full load), the system is designed to withstand the extreme conditions and thus, the corresponding calculations are

243   usually carried out at the maximum bearable (for the system) temperature of 36°C for the LT fresh water. Therefore, in

244   the present study we used this temperature set point and calculated the system pumps power demand considering

245   various operating cases (pump speed different than the baseline). This results in a demanding operating scenario for the

246   cooling system as usually the sea water temperature and the set point for the LT fresh water temperature are less and

247   therefore, greater openings of the three-way valve (in comparison with the predicted values presented below) are

248   expected.

249   The LT three-way valve temperature set point may only slightly affect the main and auxiliary engines brake specific fuel

250   consumption as it can influence the air coolers operation and up to an extent the engines scavenging air temperature.

251   However, as it is mainly adjusted to match the prevailing environmental conditions, its contribution on the ship engines

252   operation cannot readily identified. It must be noted that such an investigation is outside the scope of the present study.

253   The first investigated scenario considers the pumps operation at their rated speed, i.e. at 1200 r/min. The obtained

254   results for the operation of the M/E at four different loads (namely 25%, 50%, 75% and 100% of its MCR point)

255   considering that two D/G sets operate at 55% load in all cases are presented in Table 2. The calculations were based on

256   the constraint that the temperature difference at the coolers sides should be greater than 5°C as proposed to [16]. By

257   elaborating the results of Table 2, it can be inferred that the central cooler thermal flows (fresh water/sea water) have

258   been in adequate convergence with difference less than ±0.5% (differences lower than ±1.3% were obtained for the

259   results presented in the subsequent Tables 3-5). When the ship main engine operates at 100% load, two sea water pumps

260   and two LT fresh water pump should operate in order to satisfy the system heat demands. However, the obtained flow

261   rates for the each operating SW and LT fresh water pumps were lower than their nominal ones, which means that there

262   is adequate capacity for covering additional heat removal needs from the rest auxiliary machinery. The flow rate of the

263   HT fresh water pump is slightly lower than its nominal value as this system covers only the main engine jacket water

264   needs. The temperature differences at the central cooler sides are 6.9°C and 11°C, respectively. For the operation of M/E

265   at lower loads, one pump of each group (i.e. seawater, LT fresh water, HT fresh water) is required to cover the system

266   needs. All operating pumps run at flow rates slightly lower than their nominal values and therefore, the power demand

267   is expected to be close to the rated power, which can also be inferred by comparing the data contained in Tables 1 and 2.

268   Another point that needs attention is the pressure level of the LT and HT fresh water entering the main and auxiliary

269   engines. According to the main engine manufacturer, a typical range for the HT fresh water manometric pressure is

270   between 3.5 and 4.5 bar with the alarm limit typically being set at 2 bar. The respective typical range for the engine air

271   cooler manometric pressure is 2-4.5 bar with the low alarm lever being set at 1 bar. By taking into account that the LT

272 and HT systems expansion tanks are installed 15 m above the respective pumps suction pipes, the calculated

273 manometric pressure values for the case of 100% load main engine operation were found to be 2.55 bar for the air

274 cooler and LO cooler inlets, respectively, and 3.75 bar for the main engine HT inlet. Similar values were obtained for

275 the other investigated cases, as the pumps operating points were very close to the operating points for the 100% main

276 engine load case. As it was expected, the calculated pressure values lay within the recommended ranges for the pumps

277 operation at their nominal speed of 1200 rpm). In addition, although the engine manufacturer proposes a recommended

278 head value for the sea water pump, there is not any specific requirement for the sea water pressure level.

279 A second case was simulated considering the system pumps operation at 1100 r/min, which can be obtained by using a

280 variable speed drive. The obtained results for the operation of the M/E at four different loads (namely 25%, 50%, 75%

281 and 100% of their MCR points) considering the two D/G sets operate at 55% load are presented in Table 3. For the case

282 where the ship main engine operates at 100% load, the sea water and HT fresh water pumps can cover the system

283 requirements; however the LT fresh water pumps need to operate at their rated speed in order to satisfy the system

284 constraint (5°C temperature difference at heat exchangers sides). Furthermore, even though at full load the LT pumps

285 operate at the rated speed, their power demand is higher compared to baseline case due to the losses of the variable

286 frequency drive. However, there is a reduction in the total required power by 11.6 kWe (113.9 instead of 125.5 kWe), i.e.

287 in percentage of 9.24%. When the ship main engine operates at lower loads, one pump unit from each group is adequate

288 to cover the system needs as the total heat capacity is lower, and as a result less total power (compared to the case where

289 the main engine operates at 100% load) is required.

290 For the 25% load operation of the main engine, the manometric pressure upstream the main engine LO and air coolers

291 was calculated at 2.4 bar, whereas the a value of 3.4 bar was derived for the manometric pressure at the main engine

292 jacket circuit inlet. It can be inferred that there is a leeway for the LT pumps to operate at a lower speed, however the

293 HT pump marginally provides the required pressure level in the HT cooling water system.

294 The total required power as function of the M/E load for the two scenarios presented above is shown in Figure 6. The

295 electric power demand reduction when the pump speed is reduced lies in the region of 9.24% for the 100% main engine

296 load operation and 14.4% for operation of the main engine at lower loads. As it can be also seen in Figure 6, the total

297 power demand depends on the number of the operating pumps and their speed. In both the investigated cases, the power

298 demand is almost constant for the operation of main engine for 25% to 75% load where one pump of each group

299 operates. Therefore, it is concluded that there is potential for reducing the system power demand by using variable

300 speed drives and appropriate control of the cooling system pumps speed.

301 The system operation considering the usage of variable speed drives was simulated and the pumps speed values that

302 result in the minimum power demand were calculated for the cases of setting the constraint for the minimum

303 temperature difference at 5°C (denoted as ΔTmin1) and 10°C (denoted as ΔTmin2) at the system heat exchangers sides.

304 The former represents a realistic operating scenario, whereas the latter represents a more demanding scenario for the

305 system actual operation. The respective results are presented in Tables 4 and 5 and in Figure 7. For the former case

306 (Table 4), the system pumps speed values are considerably reduced in comparison with the baseline case, and as a result

307 the total power demand is significantly lower. For the latter case (Table 5), the power demand is higher but is still lower

308 than the one of the baseline case for M/E load lower than 75%. For operation of the ship main engine at 100% load, the

309 sea water pump must provide greater flow rate in order to satisfy the 10°C sides temperature difference constraint and

310 therefore, greater SW pump speed is needed (1380 r/min instead of 1200 r/min), which results in greater power demand.

311 With regards to the manometric pressure constrains for the main engine operation at 25% load (the rotational speed fo

312 LT and HT pumps were found to be 500 and 550 r/min, respectively), the calculated values were 1.7 bar for the LT

313 cooling system (upstream LO and air coolers) and 2 bar, respectively. Both values are outside the recommended ranges.

314 In addition, the HT system alarm will be triggered at this operating pressure level. Therefore, it can be deduced that the

315 operation of the LT and HT cooling pumps at so low rotational speed cannot be allowed, unless a change in these

316 system design is investigated. A possible solution on this is the proposal of closed pressurised expansion tanks for each

317 cooling system (industrial expansion tanks with volumes up to 15 m^3 are available).

318 Finally, the estimation of the annual energy demand of the integrated cooling system is presented in Figure 8. The

319 annual ship operating profile was taken into account as well as the ship annual sailing hours, which were estimated by

320 considering an average round trip distance of 9.000 nm, a sailing speed of 12 knots and 15% maintenance time. It is

321 inferred from the results shown in Figure 8 that there is a noteworthy potential for energy saving from the operation of

322 the cooling system if variable speed drive technologies are used on-board ships.

323
324 **Table 1 Cooling system pumps nominal characteristics**

SW pumps	Speed (r/min)	1200
	Number	2
	Rated power (kWe)	37
	Head (m)	25
	Flow rate (m^3/h)	400
LT fresh water pumps	Speed (r/min)	1200
	Number	2
	Rated power (kWe)	37
	Head (m)	30
	Flow rate (m^3/h)	350
HT fresh water pump	Speed (r/min)	1200
	Number	2
	Rated power (kWe)	15
	Head (m)	30
	Flow rate (m^3/h)	97

325
326

Table 2 Simulation results for the baseline case (1200 rpm)

Main Engine load (%)	System pumps	Pump speed (rpm)	No of operating pumps	Total electric Power (kW)	LT 3-way valve By-pass flow percentage (%)	HT 3-way valve By-pass flow percentage (%)	total flow rate (m³/h)	Central cooler inlet Temp. FW side (°C)	Central cooler outlet Temp. FW side (°C)	Central cooler outlet Temp. SW side (°C)	HTFW cooler inlet Temp. LT FW side (°C)	HTFW cooler outlet Temp. LT FW side (°C)	HTFW cooler outlet Temp. HT FW side (°C)
25	SW	1200	1	30.36	40%	60%	272.8	43.2	31.2	30.8	42.0	50.1	65.6
	LT	1200	1	35.76			210.0						
	HT	1200	1	10.49			79.0						
50	SW	1200	1	30.33	25%	50%	272.8	51.2	31.0	37.5	46.0	62.3	62.0
	LT	1200	1	36.00			213.7						
	HT	1200	1	11.05			85.8						
75	SW	1200	1	30.33	20%	35%	272.8	57.7	30.6	42.8	47.8	68.0	62.3
	LT	1200	1	36.15			214.1						
	HT	1200	1	11.27			88.55						
100	SW	1200	2	52.59	0%	0%	338.7	55.9	36.0	49.0	44.0	59.6	64.4
	LT	1200	2	61.41			390.0						
	HT	1200	1	11.51			92.7						

Table 3 Simulation results for the case where the pumps operate at 1100rpm

Main Engine load (%)	System pumps	Pump speed (rpm)	No of operating pumps	Total electric Power (kW)	LT 3-way valve By-pass flow percentage (%)	HT 3-way valve By-pass flow percentage (%)	total flow rate (m³/h)	Central cooler inlet Temp. FW side (°C)	Central cooler outlet Temp. FW side (°C)	Central cooler outlet Temp. SW side (°C)	HTFW cooler inlet Temp. LT FW side (°C)	HTFW cooler outlet Temp. LT FW side (°C)	HTFW cooler outlet Temp. HT FW side (°C)
25	SW	1100	1	25.80	30%	57%	250.0	43.8	32.6	31.4	42.8	52.6	65.4
	LT	1100	1	30.40			195.5						
	HT	1100	1	9.35			73.6						
50	SW	1100	1	25.81	20%	40%	250.0	52.6	31.9	38.7	47.2	65.0	63.5
	LT	1100	1	30.90			196.3						
	HT	1100	1	9.69			80.7						
75	SW	1100	1	25.80	16%	32%	250.0	59.6	31.1	44.5	48.9	71.0	61.5
	LT	1100	1	31.10			196.8						
	HT	1100	1	10.21			81.4						
100	SW	1100	2	44.89	0%	0%	310.0	56.0	36.0	51.0	44.0	59.7	63.0
	LT	1200	2	61.41			390.0						
	HT	1100	1	7.61			85.0						

334
335 **Table 4 Simulation results for the case of using variable speed drives for obtaining minimum system power under the constraint of 5°C allowed minimum temperature difference at heat exchanger sides(ΔTmin1)**

Main Engine load (%)	System pumps	Pump speed (rpm)	No of operating pumps	Total electric Power (kW)	LT 3-way valve By-pass flow percentage (%)	HT 3-way valve By-pass flow percentage (%)	total flow rate (m³/h)	Central cooler inlet Temp. FW side (°C)	Central cooler outlet Temp. FW side (°C)	Central cooler outlet Temp. SW side (°C)	HTFW cooler inlet Temp. LT FW side (°C)	HTFW cooler outlet Temp. LT FW side (°C)	HTFW cooler outlet Temp. HT FW side (°C)
25	SW	350	1	6.60	0%	50%	78.3	53.0	36.0	45.3	51.2	73.0	56.3
	LT	500	1	9.14			89.6						
	HT	550	1	2.66			38.4						
50	SW	600	1	8.26	0%	16%	135.3	58.6	36.0	50.2	51.3	75.7	56.1
	LT	800	1	16.20			144.0						
	HT	550	1	2.85			41.0						
75	SW	800	1	12.31	0%	0%	181.0	61.7	36.0	51.9	50.0	74.2	55.7
	LT	1000	1	24.51			180.2						
	HT	550	1	2.92			42.1						
100	SW	1100	2	45.96	0%	0%	310.0	55.9	36.0	51.0	44.0	59.7	48.9
	LT	1200	2	61.40			390.0						
	HT	600	1	3.15			46.5						

336
337
338
339 **Table 5 Simulation results for the case of using variable speed drives for obtaining minimum system power under the constraint of 10°C allowed minimum temperature difference at heat exchanger sides (ΔTmin2)**

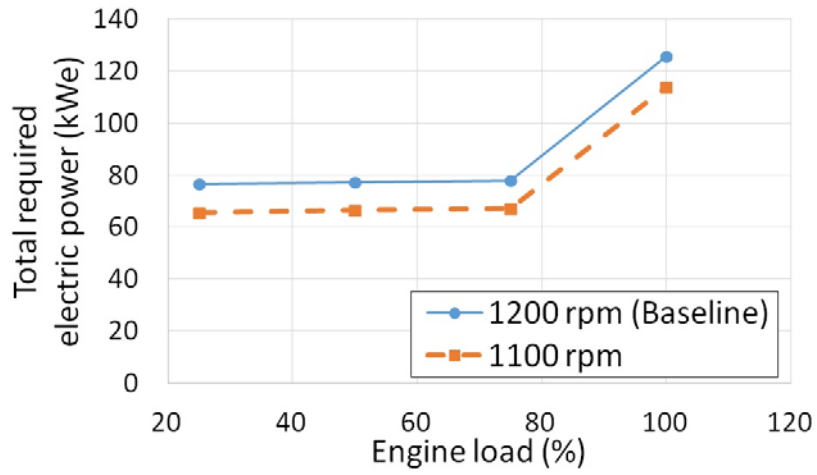| Main Engine load (%)	System pumps	Pump speed (rpm)	No of operating pumps	Total electric Power (kW)	LT 3-way valve By-pass flow percentage (%)	HT 3-way valve By-pass flow percentage (%)	total flow rate (m³/h)	Central cooler inlet Temp. FW side (°C)	Central cooler outlet Temp. FW side (°C)	Central cooler outlet Temp. SW side (°C)	HTFW cooler inlet Temp. LT FW side (°C)	HTFW cooler outlet Temp. LT FW side (°C)	HTFW cooler outlet Temp. HT FW side (°C)
25	SW	600	1	8.26	0%	42%	135.3	46.6	36.0	36.6	45.4	59.0	60.2
	LT	800	1	16.20			144.0						
	HT	550	1	2.74			39.7						
50	SW	800	1	12.28	0%	10%	181.0	54.0	36.0	44.0	48.2	67.7	58.2
	LT	1000	1	23.95			180.0						
	HT	550	1	2.74			41.5						
75	SW	1000	1	19.95	0%	0%	226.8	57.4	36.0	46.0	47.7	67.7	57.7
	LT	1200	1	36.08			216.5						
	HT	600	1	2.74			46.0						
100	SW	1380	2	90.40	0%	0%	390.0	55.9	36.0	45.8	44.0	59.8	53.6
	LT	1200	2	61.40			390.0						
	HT	700	1	5.00			54.7						

340
341

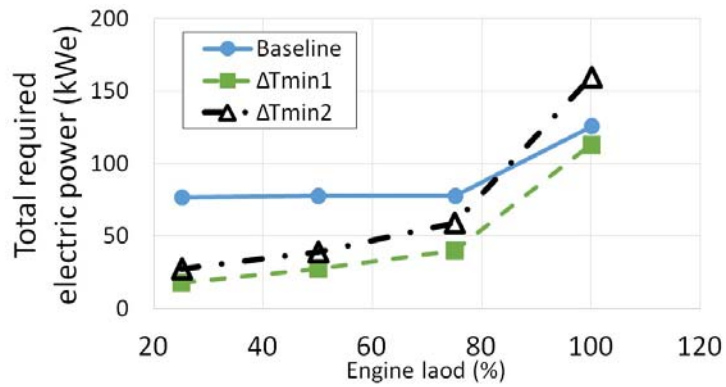Figure 6: Cooling system total electric power demand

Figure 7: Cooling system total minimum electric power demand for two different constraints of coolers sides minimum allowed temperature difference. ΔTmin1: 5°C min; ΔTmin2: 10°C.
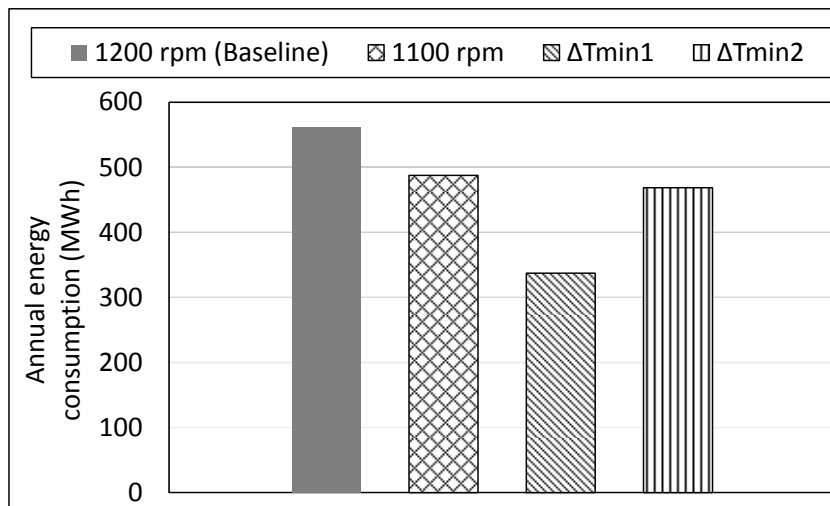

Figure 8: Annual energy consumption

356   **Conclusions**

357   The operation of the integrated sea water/ fresh water cooling system of a handymax bulk carrier was investigated

358   through simulation. Various cases of operating the system pumps including constant and variable speed were examined.

359   The main conclusions derived from this work are summarised as follows.

360   –   When the pumps operate at their rated speed the power demand is close to the rated pumps power independently of

361   the cooling system rejected heat capacity that vary with the M/E and D/G sets loading.

362   –   By reducing the pump speed the required pump power can lower, thus enabling the fuel saving.

363   –   Variable frequency drives and control of the cooling system pumps speed can result in substantial reduction of the

364   required power considering that the ship engines and machinery rarely operate at their maximum load.

365   –   There is high potential for reduction of the required power demand with the use of variable speed drives installed

366   in the ship cooling pumps, since the system is designed to cover the worse operating conditions i.e. tropical

367   conditions and maximum load of ship engines and machinery, which does not represent the actual system

368   operation.

369   –   For the LT and HT fress water cooling pumps, their minimum rotational speeds are constrained by the engine

370   manufacturer required pressure levels. For fully exploiting the energy saving capabilities in these systems,

371   alternative designs including closed expension tanks need to be further investigated.

372   The presented simulation tool and the estimation of the annual energy consumption could be used as tool for evaluating

373   the energy saving potential for the ship auxiliary systems and the techno-economic study of the installation of variable

374   frequency drives for the ship main pumps and fans.

375

376   **Acknowledgements**

380

381

References

1. IMO. (2011). *Resolution MEPC.203(62), Amendments to the annex of the protocol of 1997 to amend the international convention for the prevention of pollution from ships, 1973, as modified by the protocol of 1978 relating thereto (Inclusion of regulations on energy efficiency for ships in MARPOL Annex VI)*, MEPC 62/24/Add.1, London: International Maritime Organization.

2. ABB. (2013). *SW Cooling Pumps Variable Speed Drives Upgrade.* ABB Technical Report.

3. Su C.L., Chung W.L., Yu K.T. (2013b). *An energy-savings evaluation method for variable-frequency-drive applications on ship central cooling systems*. IEEE Transactions on Industry Applications, . 50(2), 1286-1294.

4. ABB. (2012). *Using Variable Frequency Drives (VFD) to save energy and reduce emissions in new builds and existing ships.* ABB Technical Report.

5. Mrakovcic T., Medica V., Skific N. (2004). *Numerical modelling of an engine cooling system*, Journal of Mechanical Engineering, 50(2), 104-114.

6. Hansen M., Stoustrup J., Bendtsen J. (2013). *Modeling and control of a single-phase marine cooling system*. Control Engineering Practice, 21, 1726-1734.

7. DNV GL SE, (2015). Rules for Classification and Construction, I-1.2, July 2015, Hamburg, Germany.

8. Haaland S.E. (1983). *Simple and Explicit Formulas for the Friction Factor in Turbulent Flow*. Journal of Fluids Engineering, 103 (5), 89–90.

9. Brkic D. (2011). *Review of explicit approximations to the Colebrook relation for flow friction*, Journal of Petroleum Science and Engineering, 77, 34-48.

10. Peters M.S., Timmerhais K., West R.E. (2003). *Plant Design and Economics for Chemical Engineers*, 5th ed. McGraw Hill.

11. Shah R.K., Sekulic D.P., (2003). *Fundamentals of heat exchanger design*, John Wiley & Sons.

12. Karassik I., Messina J., Cooper P., Heald C. (2001). *Pump Handbook*. Third Edition, McGraw-Hill, USA.

13. US Department of Energy. (1991). *Fact Sheet: Determining Electric Motor Load and Efficiency*. Motor Challenge Program, Technical Report.

14. Athanasiadis N. (1989). *Hydrodynamic Machinery*. NTUA, Athens.

15. Lobanoff V.S., Ross R.R. (1985). *Centrifugal Pumps Design and Application.* Gulf Publishing, Houston TX.

16. SNAME. (1990), *Marine Diesel Power Plant Practises. T&R Bulleting, No. 3-39.*.

17. Baldi F., Bengtsson S., Andersson A. (2013*). The influence of propulsion system design on the carbon footprint of different marine fuels*. Low Carbon Shipping Conference, London.

18. MAN Diesel & Turbo. (2010). *7S50MC-C8.2-TII with 1x MAN TCA66-21. Project Guide-Marine*, Augsburg, Germany.

19. MAN Diesel & Turbo. (2015). *L16/24 Project Guide – Marine Four-stroke GenSet compliant with Tier II*, Augsburg, Germany.

413   **Nomenclature**

414   **Symbols**

415   a,b,c   constants (-)

416   A   pipe cross-section area (m^2)

417   c_p specific heat at constant pressure (J/kg K)

418   D   pipe hydraulic diameter (m)

419   e/D   relative roughness (-)

420   E   energy (kWh)

421   f   friction factor (-)

422   g   gravitational acceleration (m/s^2)

423   h   head (m)

424   H   operating hours (h)

425   K   loss coefficient (-)

426   L   pipe length (m)

427   N   rotational speed (r/min)

428   P   power (W)

429   POT   percentage of time (%)

430    $\dot{Q}$ transferred heat rate (W)

431   Re   Reynolds number (-)

432   T   temperature (K)

433    $\dot{V}$ volumetric flow rate (m^3/s)

434   z   elevation (m)

435

436   **Greek symbols**

437   Δ   difference

438   η   efficiency (-)

439   ρ   fluid density (kg/m^3)

440

441   **Subscripts**

442   C   cold side

443   CC   central cooler

444   d   drive

445   hot   hot side

446   HE   heat exchanger

447   HTFW   high temperature fresh water

448   in   inlet

449   JW   jacket water

450	LT	low temperature
451	m	motor
452	ME	main engine
453	o	outlet
454	p	pump (-)
455		

456 **Abbreviations**

457	D/E	Diesel Engine
458	D/G	Diesel Generator
459	FW	Fresh Water
460	HT	High Temperature
461	JW	Jacket Water
462	LT	Low Temperature
463	MCR	maximum continuous rating
464	M/E	Main Engine
465	SW	Sea Water
466	VFD	Variable Frequency Drive